



NONLINEAR DISCRETE-CONTINUOUS MODELS IN DYNAMIC INVESTIGATIONS OF PLANE TRUSS MEMBERS

A. P I E L O R Z (WARSZAWA)

The paper presents dynamic investigations of plane trusses subject to longitudinal deformations, using nonlinear discrete-continuous models. An external excitation is applied to a rigid body located in a truss joint. In this joint, a discrete element with a spring having a nonlinear stiffness is also located. In the considerations the wave method is applied which enables to determine displacements, strains and velocities in arbitrary cross-sections of the truss members at an arbitrary time instant. Numerical calculations are performed for two nonlinear models of the plane truss in steady as well as in transient states.

1. INTRODUCTION

The considerations are concentrated on the dynamic analysis of plane trusses. Dynamic investigations of members in these trusses are performed by means of discrete-continuous models consisting of rods of continuously distributed masses, and of rigid bodies. The discussion concerns the trusses with joints idealized as hinges without friction. In such cases, truss members are subject only to longitudinal deformations, [1]. The deformation of the truss is assumed to be sufficiently small, so that the change of the geometry of the truss can be neglected. Rigid bodies in the discrete-continuous model represent elements in truss joints joining the truss members. These elements have a rather compact structures, so they may be treated as rigid bodies. The external force is applied to one of the rigid bodies and it can be described by an arbitrary function, periodic or nonperiodic. In the discrete-continuous model, additional discrete elements can be introduced. These elements consist of a spring and a damper, and they can represent the influence of additional elements connected with the truss. The spring may have a linear or nonlinear characteristic.

Linear discrete-continuous models of plane trusses are discussed in [2]. The aim of the present paper is to generalize results of the paper [2] by introducing local nonlinearities into the models studied in [2], and to investigate the influence of these nonlinearities on displacements of rod cross-sections of plane trusses. The inclusion of such types of nonlinearities is suggested by many engineering

solutions for plane trusses, [1, 3]. In the discussion the wave method, resulting from the method of characteristics, is applied, similarly to that used in [2] for linear cases.

It should be pointed out that trusses have always been subject to intensive analysis. Particularly, their static investigations have a rich and long-lasting tradition, [1, 3, 4]. Not many papers deal with dynamic investigations of truss members, e.g. [5–7]. They concern mainly impact problems in trusses with weightless joints, taking into account elastic as well as plastic materials of truss members. The obtained results are limited to very short time intervals of the order of microseconds, while in the present paper the nonlinear models of plane trusses with long-lasting loadings are studied.

2. ASSUMPTIONS, GOVERNING EQUATIONS

Consider the nonlinear discrete-continuous model of a plane truss consisting of an arbitrary number of truss members connected by rigid bodies, and of discrete elements, as shown in Fig. 1. The cross-sections of the rods are constant, and they are subject only to longitudinal deformations. It is assumed that at time instant $t = 0$, displacements and velocities of cross-sections of the truss members are equal to zero, and that the system is loaded by an external force $P(t)$. A real damping in truss members is represented by an equivalent damping applied to the ends of the members in the model. The i -th member is characterized by the Young modulus E , density ρ , length l_i and the cross-sectional area A . The j -th rigid body having mass m_j undergoes plane motion.

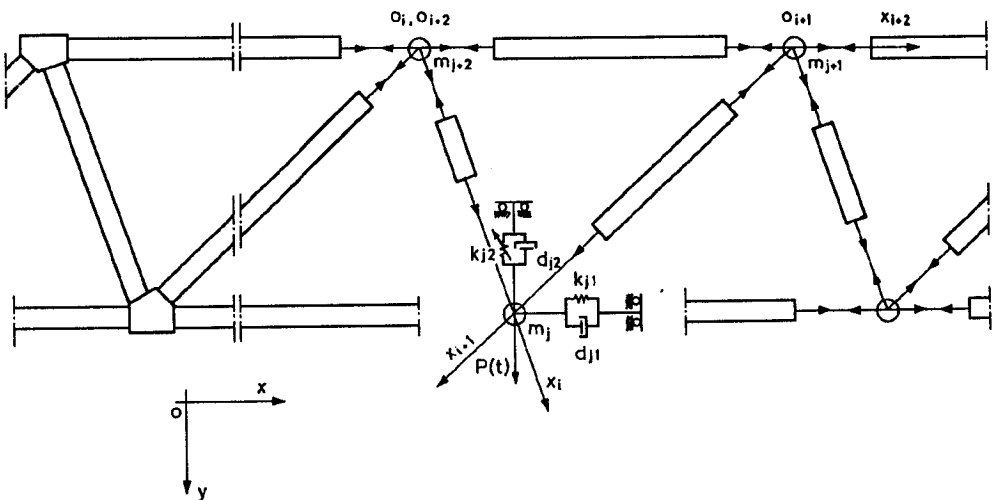


FIG. 1. Nonlinear model of a plane truss.

In the description of the nonlinear discrete-continuous model, a fixed reference system Oxy , and one-dimensional coordinate systems $O_i x_i$ assigned to individual i -th truss members are used. The origin of $O_i x_i$ system coincides with the location of one of the ends of the i -th member in the undisturbed state at $t = 0$. Displacement of the cross-section x_i in the i -th truss member is described by the function $u_i(x_i, t)$ depending on the location of the considered cross-section and on time, whereas the time functions U_j, V_j are the components of the displacements of the j -th rigid body in the x -axis and y -axis directions, respectively.

Under such assumptions, the equation of motion for the i -th truss member is the classical wave equation

$$(2.1) \quad \frac{\partial^2 u_i(x_i, t)}{\partial t^2} - a^2 \frac{\partial^2 u_i(x_i, t)}{\partial x_i^2} = 0 \quad \text{for } 0 < x_i < l_i,$$

where $a^2 = E/\rho$.

Equations with the damping continuously distributed should better describe the motion of truss members. However, no effective methods have been developed thus far for solving the appropriate equations of motion in the case of discrete-continuous models. For this reason, damping is described by an equivalent internal and external damping taken into account in the boundary conditions.

In order to find solutions of particular nonlinear cases, we must add to Eqs. (2.1) the following initial conditions

$$(2.2) \quad u_i(x_i, 0) = \frac{\partial u_i}{\partial t}(x_i, 0) = 0$$

and the appropriate nonlinear boundary conditions satisfied in truss joints. In analogy to those in [2] for the linear cases, they depend on the number of truss members in joints. For example, for the j -th joint with n truss members, the nonlinear boundary conditions may be written in the following general form:

$$(2.3) \quad \begin{aligned} & a_{1j} \frac{d^2 U_j}{dt^2} + a_{2j} \frac{dU_j}{dt} + F_{Uj}(U_j) + \sum_{k=1}^n \left(a_{3jk} \frac{\partial^2 u_i}{\partial x_i \partial t} + a_{4jk} \frac{\partial u_i}{\partial x_i} \right) = 0, \\ & b_{1j} \frac{d^2 V_j}{dt^2} + b_{2j} \frac{dV_j}{dt} + F_{Vj}(V_j) + \sum_{k=1}^n \left(b_{3jk} \frac{\partial^2 u_i}{\partial x_i \partial t} + b_{4jk} \frac{\partial u_i}{\partial x_i} \right) + P(t) = 0, \\ & u_i = u_i(u_1, u_2), \quad i = 3, 4, \dots, n, \end{aligned}$$

where a_{1j} and b_{1j} are determined by the mass m_j , a_{2j} and b_{2j} represent coefficients of external damping, a_{3jk} and b_{3jk} represent the internal damping of the Voigt type in successive truss members, a_{4jk} , b_{4jk} are determined by material

constants, and the functions F_{U_j} and F_{V_j} represent local nonlinearities in the model. In [2] F_{U_j} and F_{V_j} are linear functions.

The components U_j, V_j of the displacement of the j -th joint in the plane truss may be described by the displacements of an arbitrary pair of truss members in the joint. The conditions (2.3) are written for the case when they are determined by appropriate displacements u_1, u_2 of the first two truss members in the j -th joint. This assumption does not reduce the generality of the considerations. In analogy to static displacements, it is shown in [2] that if z_i corresponds to the displacement u_i of the end of the i -th truss member in the j -th joint, then the functions U_j, V_j and the relations needed in boundary conditions (2.3) have the form

$$(2.4) \quad \begin{aligned} U_j &= (z_k \cos \alpha_i - z_i \cos \alpha_k) \sin^{-1}(\alpha_k - \alpha_i), \\ V_j &= (z_i \sin \alpha_k - z_k \sin \alpha_i) \sin^{-1}(\alpha_k - \alpha_i), \\ z_i \sin(\alpha_2 - \alpha_1) &= z_2 \sin(\alpha_i - \alpha_1) - z_1 \sin(\alpha_i - \alpha_2), \quad i = 2, 3, \dots, n, \end{aligned}$$

where $i < k$ and α_i is the angle between the i -th truss member and the y -axis, $i = 1, 2, \dots, n$, [2]. The relations (2.4) are derived under the assumptions that the angles α_i remain constant during the motion of the truss and that z_i are orthogonal projections of the displacements of the ends of the i -th truss members. The truss members undergo small deformations and small displacements, so the above assumptions are justified, [2].

Taking into account initial conditions (2.2), one could assume the solution of Eqs. (2.1) in the form

$$(2.5) \quad u_i(x_i, t) = f_i(a(t - t_{f_i}) - x_i + x_{f_i}) + g_i(a(t - t_{g_i}) + x_i - x_{g_i}),$$

where the functions f_i, g_i represent disturbances caused by the external force $P(t)$ in the i -th truss member in the directions consistent with and opposite to the direction of the x -axis, respectively. Constants $t_{f_i}, t_{g_i}, x_{f_i}, x_{g_i}$ in the arguments of these functions denote the time instant and the location of the end of the i -th member in which the first disturbance is observed. These constants may be equal or differ from each other. The functions f_i, g_i are continuous functions of a single variable, and for negative arguments they are identically equal to zero. Their forms are determined by the boundary conditions of particular problems. Upon substituting the solution (2.5) into appropriate nonlinear boundary conditions, nonlinear ordinary differential equations with retarded arguments are obtained for unknown functions f_i, g_i .

The approach described above can be used for the consideration of complex nonlinear discrete-continuous models similar to that shown in Fig. 1. However, in the present paper, detailed investigations are made for two specific portions

of the plane truss. It should be pointed out that nonlinear discrete-continuous models of trusses have not been known in the available literature. Moreover, simple nonlinear models lead to the solution of a smaller number of nonlinear equations, and in spite of simplification they can give useful information on the dynamic behaviour of nonlinear models of plane trusses.

The characteristic of nonlinear springs in the discrete-continuous models is assumed to be of a hard type. In the paper, the force acting in the spring is described by the function

$$(2.6) \quad F(X) = K_1X + K_3X^3 \quad \text{with } K_3 \geq 0,$$

where, according to (2.3) $X = U_j$ or $X = V_j$. The nonlinear functions of the type (2.6) are exploited widely in dynamic investigations of nonlinear discrete systems, [8].

3. PARTICULAR CASES OF NONLINEAR MODELS OF A PLANE TRUSS

Real trusses usually consist of repeated portions. Below, we discuss two nonlinear models of portions where the influence of adjoining truss portions are taken into account by means of discrete elements consisting of a spring and a damper. It is assumed that one of the springs has a nonlinear stiffness. The studied nonlinear models differ from linear models considered in [2] by a nonlinear spring located in the joint where an external load is applied.

The nonlinear model of a truss portion is shown in Fig. 2. It consists of 3 truss members having lengths l_1, l_2, l_3 . This model may be treated as a part of

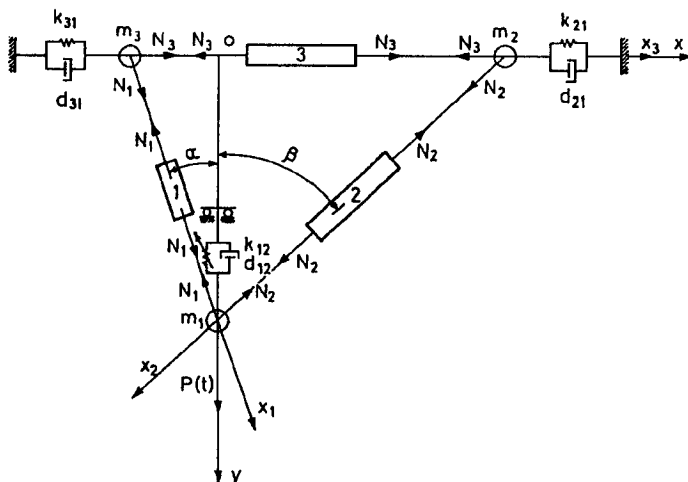


FIG. 2. Nonlinear discrete-continuous model of the portion of a plane truss.

the model of the plane truss shown in Fig. 1. In the description of the model we use a fixed reference system $0xy$ and one-dimensional coordinate systems $0_i x_i$ assigned to individual members, $i = 1, 2, 3$. The truss members (1), (2) and the y -axis make angles α , β , respectively.

In the model, a rigid body m_1 is located in the joint with coordinates $x = 0$, $y = l_1 \cos \alpha$ ($x_1 = l_1$, $x_2 = l_2$). It is loaded by an external force $P(t)$ acting parallel to the y -axis. The force and the reaction displace the rigid body m_1 in the plane xy . For simplicity, it is assumed that the displacement of this rigid body in the x -axis direction is equal to zero ($U_1 \equiv 0$, $V_1 \neq 0$). The rigid body m_1 is connected with a nonlinear discrete element, with the nonlinear stiffness of the spring $k_{12}(V_1) = F_{V_1}(V_1)/V_1$ and with the damping coefficient d_{12} . The rigid body m_2 is located in the joint of coordinates $x = l_2 \sin \beta$, $y = 0$ ($x_2 = 0$, $x_3 = l_3$). It displaces only along the x -axis ($U_2 \neq 0$, $V_2 \equiv 0$). A discrete element with coefficients k_{21} , d_{21} representing the effect of additional elements connected with the truss, is attached to this body. It is assumed that the rigid body m_3 moving only along the x -axis ($U_3 \neq 0$, $V_3 \equiv 0$) is located in the joint $x = -l_1 \sin \alpha$, $y = 0$ ($x_1 = 0$, $x_3 = 0$). A discrete element with coefficients k_{31} and d_{31} is attached to the rigid body m_3 .

As a second nonlinear model of truss portions, we consider a model described above in the case when the mass m_3 is equal to zero and the ends of members (1) and (3) in the joint $x = -l_1 \sin \alpha$, $y = 0$ are fixed. The suitable model results from Fig. 2 and for this reason it is not shown in the present paper, see [2].

The models considered in the paper have joints with two truss members. In such cases the relations (2.4), valid for n -member joints, reduce to

$$(3.1) \quad \begin{aligned} U_j &= (z_1 \cos \beta - z_2 \cos \alpha) \sin^{-1}(\alpha + \beta), \\ V_j &= (z_1 \sin \beta + z_2 \sin \alpha) \sin^{-1}(\alpha + \beta) \quad \text{for } \alpha_1 = \alpha, \quad \alpha_2 = 2\pi - \beta, \end{aligned}$$

and

$$(3.2) \quad U_j = z_1, \quad V_j = (z_2 - z_1 \sin \beta) \cos^{-1} \beta \quad \text{for } \alpha_1 = \pi/2, \quad \alpha_2 = \beta.$$

The above relations are used in formulation of the boundary conditions for the particular nonlinear models studied in the paper. Moreover, in the analogy to (2.6) the force acting in the nonlinear spring is assumed in the form

$$(3.3) \quad F(V_1) = K_{121}V_1 + K_{123}V_1^3 \quad \text{with } K_{123} \geq 0.$$

Below, solutions for two nonlinear models are presented together with appropriate numerical results.

4. SOLUTION FOR THE NONLINEAR MODEL I

The first nonlinear model discussed in the paper is that shown in Fig. 2. If one takes into account Eqs. (2.1)–(2.6) and (3.1)–(3.3), the determination of displacements for truss members (1)–(3) of the Model I is reduced to solving the equations

$$(4.1) \quad \frac{\partial^2 u_i(x_i, t)}{\partial t^2} - a^2 \frac{\partial^2 u_i(x_i, t)}{\partial x_i^2} = 0 \quad \text{for } i = 1, 2, 3$$

with initial conditions

$$(4.2) \quad u_i(x_i, 0) = \frac{\partial u_i}{\partial t}(x_i, 0) = 0 \quad \text{for } i = 1, 2, 3$$

and the following nonlinear boundary conditions

$$(4.3) \quad \begin{aligned} & -m_3 \frac{\partial^2 u_3}{\partial t^2} - d_{31} \frac{\partial u_3}{\partial t} - k_{31} u_3 + AE \left[D_3 \frac{\partial^2 u_3}{\partial x_3 \partial t} + \frac{\partial u_3}{\partial x_3} \right] \\ & \quad + AE \sin \alpha \left[D_1 \frac{\partial^2 u_1}{\partial x_1 \partial t} + \frac{\partial u_1}{\partial x_1} \right] = 0 \quad \text{for } x_1 = x_3 = 0, \\ & -u_3 \sin \beta + u_1 = 0 \quad \text{for } x_1 = x_3 = 0, \\ & u_1 \cos \beta - u_2 \cos \alpha = 0 \quad \text{for } x_1 = l_1, \quad x_2 = l_2, \\ & -m_1 \left[C_2 \frac{\partial^2 u_1}{\partial t^2} + C_1 \frac{\partial^2 u_2}{\partial t^2} \right] - d_{12} \left[C_2 \frac{\partial u_1}{\partial t} + C_1 \frac{\partial u_2}{\partial t} \right] - K_{121}(C_2 u_1 + C_1 u_2) \\ & \quad - K_{123}(C_2 u_1 + C_1 u_2)^3 - AE \cos \alpha \left[D_1 \frac{\partial^2 u_1}{\partial x_1 \partial t} + \frac{\partial u_1}{\partial x_1} \right] \\ & - AE \cos \beta \left[D_2 \frac{\partial^2 u_2}{\partial x_2 \partial t} + \frac{\partial u_2}{\partial x_2} \right] + P(t) = 0 \quad \text{for } x_1 = l_1, \quad x_2 = l_2, \\ & -m_2 \frac{\partial^2 u_3}{\partial t^2} - d_{21} \frac{\partial u_3}{\partial t} - k_{21} u_3 - AE \left[D_3 \frac{\partial^2 u_3}{\partial x_3 \partial t} + \frac{\partial u_3}{\partial x_3} \right] \\ & \quad - AE \sin \beta \left[D_2 \frac{\partial^2 u_2}{\partial x_2 \partial t} + \frac{\partial u_2}{\partial x_2} \right] = 0 \quad \text{for } x_2 = 0, \quad x_3 = l_3, \\ & u_3 \sin \beta + u_2 = 0 \quad \text{for } x_2 = 0, \quad x_3 = l_3, \end{aligned}$$

where

$$(4.4) \quad C_1 = \frac{\sin \alpha}{\sin \xi}, \quad C_2 = \frac{\sin \beta}{\sin \xi}, \quad \xi = \alpha + \beta.$$

Upon the introduction of nondimensional quantities

$$(4.5) \quad \begin{aligned} \bar{x}_i &= x_i/l_0, & \bar{t} &= at/l_0, & \bar{u}_i &= u_i/u_0, & \bar{d}_{ij} &= d_{ij}l_0/(am_0), \\ \bar{D}_i &= aD_i/l_0, & R_i &= m_i/m_0, & K_0 &= A\rho l_0/m_0, \\ \bar{P} &= Pl_0^2/(m_0u_0a^2), & \bar{k}_{ij} &= k_{ij}l_0^2/(m_0a^2), & \bar{l}_i &= l_i/l_0, \\ \bar{K}_{121} &= K_{121}l_0^2/(m_0a^2), & \bar{K}_{123} &= K_{123}u_0^2l_0^2/(m_0a^2), & \bar{p} &= pl_0/a, \end{aligned}$$

relations (4.1)–(4.3) take the form

$$(4.6) \quad \frac{\partial^2 u_i(x_i, t)}{\partial t^2} - \frac{\partial^2 u_i(x_i, t)}{\partial x_i^2} = 0 \quad \text{for } i = 1, 2, 3,$$

$$(4.7) \quad u_i(x_i, 0) = \frac{\partial u_i}{\partial t}(x_i, 0) = 0 \quad \text{for } i = 1, 2, 3,$$

$$(4.8) \quad \begin{aligned} & -R_3 \frac{\partial^2 u_3}{\partial t^2} - d_{31} \frac{\partial u_3}{\partial t} - k_{31} u_3 + K_0 \left[D_3 \frac{\partial^2 u_3}{\partial x_3 \partial t} + \frac{\partial u_3}{\partial x_3} \right] \\ & \quad + K_0 \sin \alpha \left[D_1 \frac{\partial^2 u_1}{\partial x_1 \partial t} + \frac{\partial u_1}{\partial x_1} \right] = 0 \quad \text{for } x_1 = x_3 = 0, \\ & -u_3 \sin \beta + u_1 = 0 \quad \text{for } x_1 = x_3 = 0, \\ & u_1 \cos \beta - u_2 \cos \alpha = 0 \quad \text{for } x_1 = l_1, \quad x_2 = l_2, \\ & -R_1 \left[C_2 \frac{\partial^2 u_1}{\partial t^2} + C_1 \frac{\partial^2 u_2}{\partial t^2} \right] - d_{12} \left[C_2 \frac{\partial u_1}{\partial t} + C_1 \frac{\partial u_2}{\partial t} \right] - K_{121}(C_2 u_1 + C_1 u_2) \\ & \quad - K_{123}(C_2 u_1 + C_1 u_2)^3 - K_0 \cos \alpha \left[D_1 \frac{\partial^2 u_1}{\partial x_1 \partial t} + \frac{\partial u_1}{\partial x_1} \right] \\ & - K_0 \cos \beta \left[D_2 \frac{\partial^2 u_2}{\partial x_2 \partial t} + \frac{\partial u_2}{\partial x_2} \right] + P(t) = 0 \quad \text{for } x_1 = l_1, \quad x_2 = l_2, \\ & -R_2 \frac{\partial^2 u_3}{\partial t^2} - d_{21} \frac{\partial u_3}{\partial t} - k_{21} u_3 - K_0 \left[D_3 \frac{\partial^2 u_3}{\partial x_3 \partial t} + \frac{\partial u_3}{\partial x_3} \right] \\ & \quad - K_0 \sin \beta \left[D_2 \frac{\partial^2 u_2}{\partial x_2 \partial t} + \frac{\partial u_2}{\partial x_2} \right] = 0 \quad \text{for } x_2 = 0, \quad x_3 = l_3, \\ & u_3 \sin \beta + u_2 = 0 \quad \text{for } x_2 = 0, \quad x_3 = l_3, \end{aligned}$$

where overbars are omitted for convenience, and l_0 , u_0 , m_0 , are fixed values of the length, displacement and mass, respectively.

According to (2.5), the solutions of Eqs. (4.6), taking into account (4.7), are sought in the form

$$(4.9) \quad \begin{aligned} u_1(x_1, t) &= f_1(t - x_1 + l_1) + g_1(t + x_1 - l_1), \\ u_2(x_2, t) &= f_2(t - x_2 + l_2) + g_2(t + x_2 - l_2), \\ u_3(x_3, t) &= f_3(t - l_1 - x_3) + g_3(t - l_2 + x_3 - l_3), \end{aligned}$$

where functions f_i and g_i represent waves propagating in the i -th truss member in a direction consistent with and opposite to the x -axis direction, respectively. In the considered model, the disturbances caused by the external force $P(t)$ arrive to the member (3) through the member (1) as well as through the member (2). Thus, according to (2.5), it is taken into account in (4.9) that $t_{f_3} = l_1$ and $x_{f_3} = 0$ while $t_{g_3} = l_2$ and $x_{g_3} = l_3$.

Substituting (4.9) into the nonlinear boundary conditions (4.8), and denoting the largest argument of functions appearing in each equality by z , one obtains the following equations for 6 unknown functions $f_i, g_i, i = 1, 2, 3$,

$$(4.10) \quad \begin{aligned} f_1(z) &= -g_1(z - 2l_1) + [f_3(z - 2l_1) + g_3(z - l_1 - l_2 - l_3)] \sin \beta, \\ f_2(z) &= -g_2(z - 2l_2) - [f_3(z - l_1 - l_2 - l_3) + g_3(z - 2l_2)] \sin \beta, \\ r_1 g_1''(z) &= P(z) + r_2 g_1'(z) + r_3 f_1''(z) + r_4 f_1'(z) + r_5 f_2''(z) + r_6 f_2'(z) \\ &\quad + r_7 [f_1(z) + g_1(z)] + r_8 [f_1(z) + g_1(z)]^3, \\ g_2(z) &= -f_2(z) + [f_1(z) + g_1(z)] \cos \beta / \cos \alpha, \\ r_9 g_3''(z) + r_{10} g_3'(z) + r_{11} g_3(z) &= r_{12} f_3''(z - l_1 + l_2 - l_3) + r_{13} f_3'(z - l_1 + l_2 - l_3) \\ &\quad + r_{14} f_3(z - l_1 + l_2 - l_3) + r_{15} g_2''(z) + r_{16} g_2'(z), \\ r_{17} f_3''(z) + r_{18} f_3'(z) + r_{19} f_3(z) &= r_{20} g_3''(z + l_1 - l_2 - l_3) + r_{21} g_3'(z + l_1 - l_2 - l_3) \\ &\quad + r_{22} g_3(z + l_1 - l_2 - l_3) + r_{23} g_1''(z) + r_{24} g_1'(z), \end{aligned}$$

where

$$(4.11) \quad \begin{aligned} r_1 &= R_1 / \cos \alpha + K_0(D_1 \cos \alpha + D_2 \cos^2 \beta / \cos \alpha), \\ r_2 &= -d_{12} / \cos \alpha - K_0(\cos \alpha + \cos^2 \beta / \cos \alpha), \\ r_3 &= -R_1 / \cos \alpha + K_0(D_1 \cos \alpha - D_2 \cos^2 \beta / \cos \alpha), \\ r_4 &= -d_{12} / \cos \alpha + K_0(\cos \alpha - \cos^2 \beta / \cos \alpha), \\ r_5 &= 2K_0 D_2 \cos \beta, \quad r_6 = 2K_0 \cos \beta, \\ r_7 &= -K_{121} / \cos \alpha, \quad r_8 = -K_{123} / \cos^3 \alpha, \\ r_9 &= R_2 + K_0(D_3 + D_2 \sin^2 \beta), \quad r_{10} = d_{21} + K_0(1 + \sin^2 \beta), \\ r_{11} &= k_{21}, \quad r_{12} = -R_2 + K_0(D_3 - D_2 \sin^2 \beta), \\ r_{13} &= -d_{21} + K_0(1 - \sin^2 \beta), \quad r_{14} = -k_{21}, \end{aligned}$$

$$\begin{aligned}
 (4.11) \quad & r_{15} = -2K_0 D_2 \sin \beta, \quad r_{16} = -2K_0 \sin \beta, \\
 [\text{cont.}] \quad & r_{17} = R_3 + K_0(D_1 \sin \alpha \sin \beta + D_3), \\
 & r_{18} = d_{31} + K_0(\sin \alpha \sin \beta + 1), \quad r_{19} = k_{31}, \\
 & r_{20} = -R_3 + K_0(D_3 - D_1 \sin \alpha \sin \beta), \\
 & r_{21} = -d_{31} + K_0(1 - \sin \alpha \sin \beta), \quad r_{22} = -k_{31}, \\
 & r_{23} = 2K_0 D_1 \sin \alpha, \quad r_{24} = 2K_0 \sin \alpha.
 \end{aligned}$$

Equations (4.10) consist of one nonlinear equation and five linear equations. Linear equations are solved by the method of finite differences, and the nonlinear equation for the function $g_1(z)$ - by means of the Runge-Kutta method. Having obtained the functions f_i, g_i and their derivatives, one can determine the displacements, strains and velocities in arbitrary cross-sections at an arbitrary time instant.

The external force $P(t)$ occurring in (4.10) can be described by an arbitrary function of time. In the paper it is taken in the form

$$(4.12) \quad P(t) = P_0 \sin(pt)$$

where p is the loading frequency.

In numerical calculations, the following dimensional quantities are assumed, [2, 3],

$$\begin{aligned}
 (4.13) \quad & l_0 = l_1 = l_2 = l_3 = 2\text{m}, \quad A = 2 \cdot 10^{-3} \text{m}^2, \quad \rho = 0.8 \cdot 10^4 \text{kg/m}^3, \\
 & E = 2.1 \cdot 10^{11} \text{N/m}^2, \quad k_{ij} = K_{121} = 2.1 \cdot 10^8 \text{N/m}, \quad m_1 = 20 \text{kg}, \\
 & m_2 = m_3 = 3.2 \text{kg}, \quad m_0 = 32 \text{kg}, \quad a = 5000 \text{m/s}, \\
 & P_0 = 200 \text{kN}, \quad u_0 = 10^{-3} \text{m}, \quad \alpha = \beta = \pi/6.
 \end{aligned}$$

Then, nondimensional quantities according to (4.5) are

$$\begin{aligned}
 (4.14) \quad & R_1 = 0.625, \quad R_2 = R_3 = 0.1, \quad \bar{l}_i = 1.0, \\
 & K_0 = 1.0, \quad \bar{P}_0 = 1.0, \quad \bar{k}_{ij} = \bar{K}_{121} = 1.05.
 \end{aligned}$$

The efficiency of the method applied in the paper is demonstrated in [2] for linear models of plane trusses giving the spatial diagrams of displacements in truss members and investigating the effect of various parameters describing the considered models.

For this reason, in numerical calculations we concentrate here on the presentation of the influence of local nonlinearity on the displacements in selected cross-sections.

For parameters (4.14) and damping coefficients $d_{ij} = D_k = d_0 = 0.1$, displacements of the truss members (1), (2) are equal if $x_1 = x_2$, and displacements in the member (3) are antisymmetric with respect to the cross-section $x_3 = 0.5$.

At the beginning, the diagrams of displacements in cross-sections $x_1 = x_2 = 0, 0.5, 1$ of members (1), (2) for $p = 1.37$ and $K_{123} = 0, 0.0125$ in the steady state ($t > 970$) are plotted in Fig. 3. The frequency of the external force $p = 1.37$ corresponds to the first resonant frequency for the linear case. For the assumed parameters, amplitudes of displacements in members (1) and (2) increase with the increase of x_1, x_2 . Similar diagrams can be drawn for suitable displacements of cross-sections of member (3).

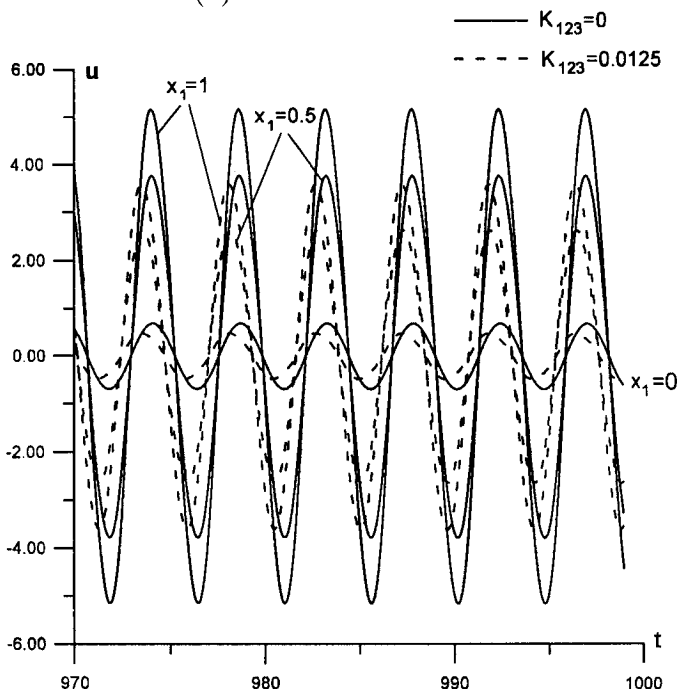


FIG. 3. Displacements of cross-sections $x_1 = x_2 = 0, 0.5, 1$ of members (1), (2) in the nonlinear Model I for $p = 1.37$ and $K_{123} = 0, 0.0125$ in the steady state.

Below, the effect of local nonlinearity is studied on the example of amplitude-frequency curves. In order to determine the suitable amplitude-frequency curves, equations (4.10) are solved from $z = 0$ until the steady state for the displacements expressed by (4.9) is reached or for the dynamic force $F(V_1)$ described by (3.3), with zero initial conditions for the functions f_i, g_i and their derivatives. Then, for every frequency p of the external force $P(t)$ there exists a value p_0 for which displacement amplitudes jump from the upper to lower curves. However, equations with a retarded argument (4.10) can be also solved with nonzero initial conditions. Nonzero values of the functions $f_i(z), g_i(z)$ and their derivatives

should be known in the interval $\langle -L, 0 \rangle$, where L is equal to the maximum shift in arguments of all functions appearing in (4.10), because (4.10) are equations with a retarded argument. If equations (4.10) with $p > p_0$ are solved up to $z_n = 2\pi m / (p_0 + n\Delta p)$, $n = 1, 2, \dots$ and m is a fixed integer, and next the values of the functions $f_i(z)$, $g_i(z)$ and their derivatives from the interval $\langle z_n - L, z_n \rangle$ are assumed to be initial values of these functions in the interval $\langle -L, 0 \rangle$ for $p = p_0 + (n + 1)\Delta p$, then the amplitudes of the sought quantities with these initial conditions lie at the extension of the upper amplitude-frequency curves up to the next jump.

From Fig. 3 it follows that the effect of local nonlinearity can be investigated for an arbitrary cross-section of the considered truss members. In order to avoid too many diagrams, we concentrate on the study of this effect on displacements V_1 of the rigid body m_1 located in the joint $x = 0$, $y = l_1 \cos \alpha$ ($x_1 = l_1$, $x_2 = l_2$). The displacement V_1 is expressed by (3.1)₂ with $z_1 = u_1(l_1, t)$, $z_2 = u_2(l_2, t)$, $\alpha_1 = \alpha$, $\alpha_2 = 2\pi - \beta$.

The effect of the assumed nonlinearity is represented by the parameter K_{123} standing at the nonlinear term in (3.3) and by the change of damping coefficient d_0 and the change of the amplitude P_0 of the external force (4.12). For this reason, in numerical calculations the effect of these parameters is studied.

In Fig. 4 are plotted the amplitude-frequency curves for displacements V_1 of the rigid body m_1 for the linear case as well as for the nonlinear model with

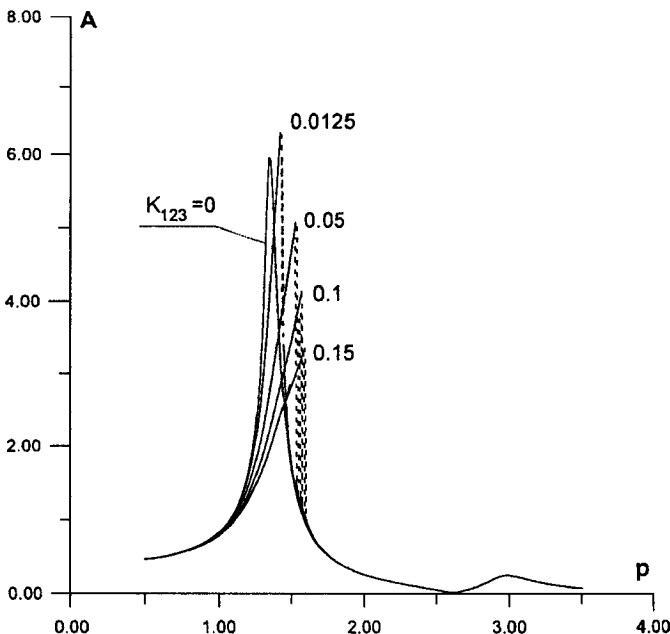


FIG. 4. Amplitude-frequency curves for displacements V_1 of the rigid body m_1 in the nonlinear Model I for $K_{123} = 0, 0.0125, 0.05, 0.1, 0.15$.

$K_{123} = 0.0125, 0.05, 0.1, 0.15$ in the first two resonant regions, $p < 3.5$. The effect of nonlinearity is noticed only in the first resonant region. It is characterized by the increase of the slope of the curves with respect to the p -axis with increasing coefficient K_{123} , and by the jump of amplitudes typical for nonlinear discrete systems described by Duffing's equation. For the assumed parameters, no large differences between the frequencies of the external loading, at which the amplitude jumps occur, are obtained. One can notice that for $K_{123} = 0.0125$ maximal amplitudes are larger than those for the linear case with $K_{123} = 0$. So, the effect of K_{123} on the displacements is not so regular as in [9] where a torsional mechanical system is discussed.

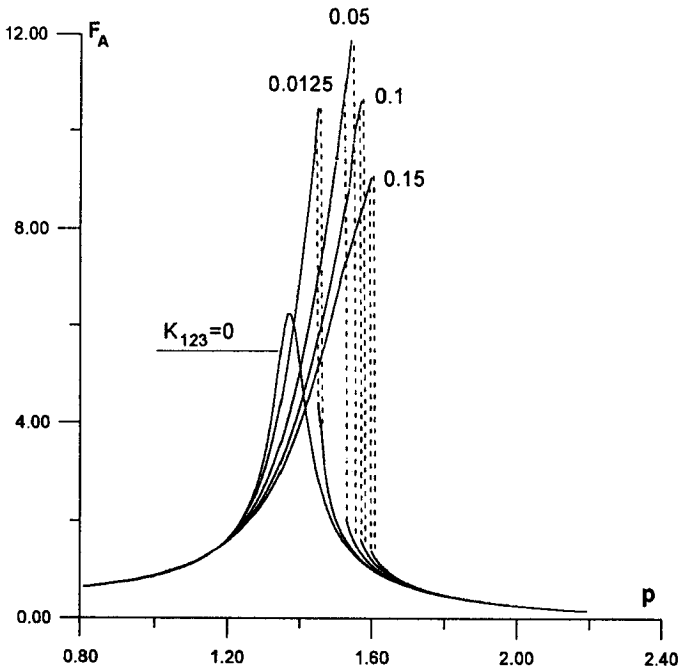


FIG. 5. Amplitude-frequency curves for dynamic force $F(V_1)$ in the nonlinear Model I for $K_{123} = 0, 0.0125, 0.05, 0.1, 0.15$.

Amplitude-frequency curves for the dynamic force $F(V_1)$ expressed by (3.3) are plotted in Fig. 5 for $K_{123} = 0, 0.0125, 0.05, 0.1, 0.15$ in the first resonant region, $p < 2.2$. From Fig. 5 it follows that maximum amplitudes for dynamic forces in the assumed nonlinear cases are considerably higher than the corresponding amplitude for the linear case.

Diagrams in Figs. 3–5 are obtained for the damping coefficients $d_0 = d_{ij} = D_k = 0.1$. The effect of the damping coefficient d_0 on displacement V_1 is shown in Fig. 6. One can notice that the increase of damping causes the decrease of the maximum amplitudes of the displacements V_1 . Moreover, the results for $d_0 = 0.3$

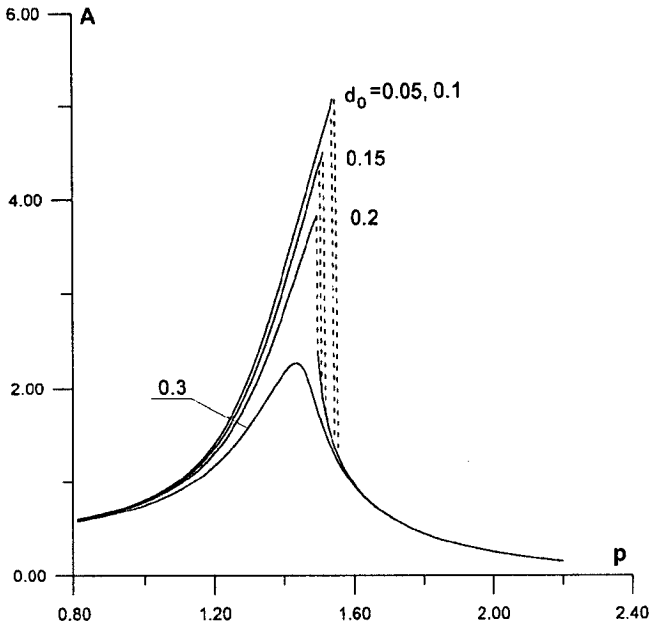


FIG. 6. Effect of damping on amplitudes of displacements V_1 in the nonlinear Model I for $d_0 = 0.05, 0.1, 0.15, 0.2, 0.3$ and $K_{123} = 0.05$.

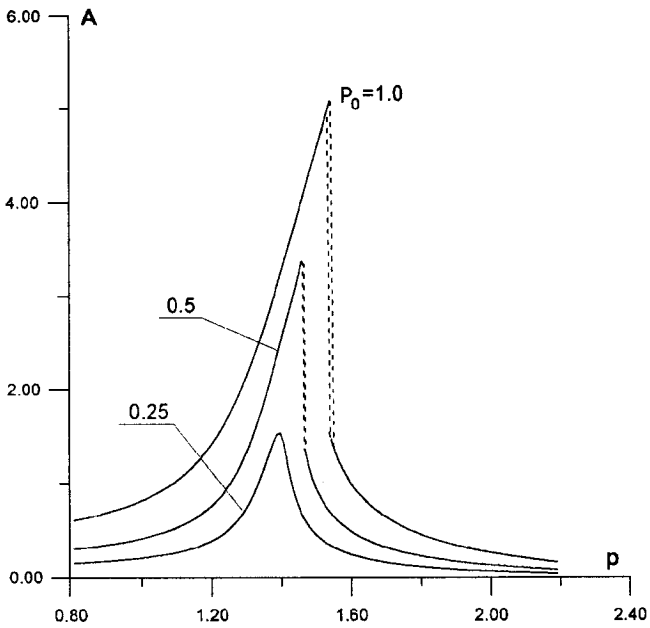


FIG. 7. Effect of amplitude P_0 of the external loading on amplitudes of displacements V_1 in the Model I with $P_0 = 0.25, 0.5, 1.0$ and $K_{123} = 0.05$.

correspond to the linear case when the jumps of displacement amplitudes do not occur.

Diagrams in Figs. 3–6 are obtained for $P_0 = 1.0$. The effect of amplitude P_0 of the external force $P(t)$ on displacements V_1 is shown in Fig. 7 for $P_0 = 0.25, 0.5, 1.0$, with $K_{123} = 0.05$ and $d_0 = 0.1$. From Fig. 7 it follows that with the decrease of the values of P_0 , the maximum displacement amplitudes also decrease. Moreover, the value $P_0 = 0.25$ corresponds to the linear case. Such a value of the amplitude of the external force (4.12) is assumed in numerical calculations presented in paper [2] where linear models of the portions of plane trusses are studied.

From Figs. 4, 6, 7 it also follows that if the nondimensional displacements V_1 are smaller than 1.0, then the considered nonlinear models with local nonlinearity and the characteristic of the spring of the hard type may be replaced by linear models.

5. SOLUTION FOR THE NONLINEAR MODEL II

The Model II differs from the Model I shown in Fig. 3 as far as the conditions in the joint $x = -l_1 \sin \alpha$, $y = 0$ ($x_1 = x_3 = 0$) are concerned. Now, the rigid body m_3 is neglected, and the ends of members (1) and (3) are fixed. In the linear case this model corresponds to the Model I in [2].

The determination of displacements of truss members in the nonlinear Model II is reduced to solving the equations of motion (4.1) with initial conditions (4.2), with boundary conditions (4.3)₃ – (4.3)₆, and with two additional boundary conditions

$$(5.1) \quad \begin{aligned} u_1(x_1, t) &= 0 & \text{for } x_1 &= 0, \\ u_3(x_3, t) &= 0 & \text{for } x_3 &= 0. \end{aligned}$$

In nondimensional quantities (4.5) the problem leads to solving equations (4.6) with (4.7), (4.8)₃ – (4.8)₆, and with (5.1) in the unchanged form because bars denoting nondimensional quantities are omitted for convenience.

Now, the solution of Eqs. (4.6) are sought in the form

$$(5.2) \quad \begin{aligned} u_1(x_1, t) &= f_1(t - x_1 + l_1) + g_1(t + x_1 - l_1), \\ u_2(x_2, t) &= f_2(t - x_2 + l_2) + g_2(t + x_2 - l_2), \\ u_3(x_3, t) &= f_3(t - l_2 - x_3 + l_3) + g_3(t - l_2 + x_3 - l_3). \end{aligned}$$

Comparing the solution (4.9) for the nonlinear Model I with the solution (5.2) one can notice that these solutions differ only in arguments of the function f_3 . Now, according to (2.5) $t_{f_3} = t_{g_3} = l_2$ and $x_{f_3} = x_{g_3} = l_3$.

Substituting (5.2) into the boundary conditions (5.1), (4.8)₃ – (4.8)₆, and denoting the largest argument of functions appearing in each equality by z , one obtains the following equations for unknown functions $f_i, g_i, i = 1, 2, 3$,

$$\begin{aligned}
 f_1(z) &= -g_1(z - 2l_1), \\
 f_2(z) &= -g_2(z - 2l_2) - [f_3(z - 2l_2) + g_3(z - 2l_2)] \sin \beta, \\
 f_3(z) &= -g_3(z - 2l_3), \\
 (5.3) \quad r_1 g_1''(z) &= P(z) + r_2 g_1'(z) + r_3 f_1''(z) + r_4 f_1'(z) + r_5 f_2''(z) + r_6 f_2'(z) \\
 &\quad + r_7 [f_1(z) + g_1(z)] + r_8 [f_1(z) + g_1(z)]^3, \\
 g_2(z) &= -f_2(z) + [f_1(z) + g_1(z)] \cos \beta / \cos \alpha, \\
 r_9 g_3''(z) + r_{10} g_3'(z) + r_{11} g_3(z) &= r_{12} f_3''(z) + r_{13} f_3'(z) \\
 &\quad + r_{14} f_3(z) + r_{15} g_2''(z) + r_{16} g_2'(z),
 \end{aligned}$$

where constants $r_i, i = 1, 2, \dots, 16$, are defined by (4.11).

The numerical examples using Eqs. (5.3) are presented for parameters (4.14) with $R_3 = 0$. Though the method applied in the paper allows to determine displacements in arbitrary cross-sections of the members of the considered nonlinear Model II, for the sake of clarity in the numerical examples the displacements V_1 of the rigid body m_1 in the steady state are determined. The external force is assumed in the form (4.12).

In Fig. 8 the amplitude-frequency curves for displacements V_1 are plotted for the frequency of the external force $p < 4.0$ with the coefficient multiplying the nonlinear term in (3.3) equal to $K_{123} = 0, 0.0125, 0.05, 0.1, 0.15$. From Fig. 8 it follows that in the interval $p < 4.0$, three resonant regions are included while for the nonlinear Model I we had only two resonant regions for this interval of p . Next, in the first resonant region one can observe the increase of the slope of the obtained curves with the increase of the value of the parameter K_{123} . For $K_{123} = 0.0125$ the largest values of amplitudes are obtained, larger than those in the linear case and for the remaining K_{123} in nonlinear cases. The jump phenomena typical for nonlinear discrete systems occur only in the first resonant region. In further resonant regions numerical results coincide with the corresponding results for the linear case.

The effect of the coefficient K_{123} on the amplitudes of forces $F(V_1)$ defined by (3.3) is shown in Fig. 9 in two resonant regions, $p < 2.3$. From diagrams in Fig. 9 it follows that the jump phenomena are also observed only in the first resonant region.

Diagrams in Figs. 8 and 9 are determined for damping coefficients $d_0 = d_{ij} = D_k = 0.1$ and the amplitude of the external force equal to $P_0 = 1.0$. The effect of parameters d_0 and P_0 on the displacements V_1 of the rigid body m_1 is shown

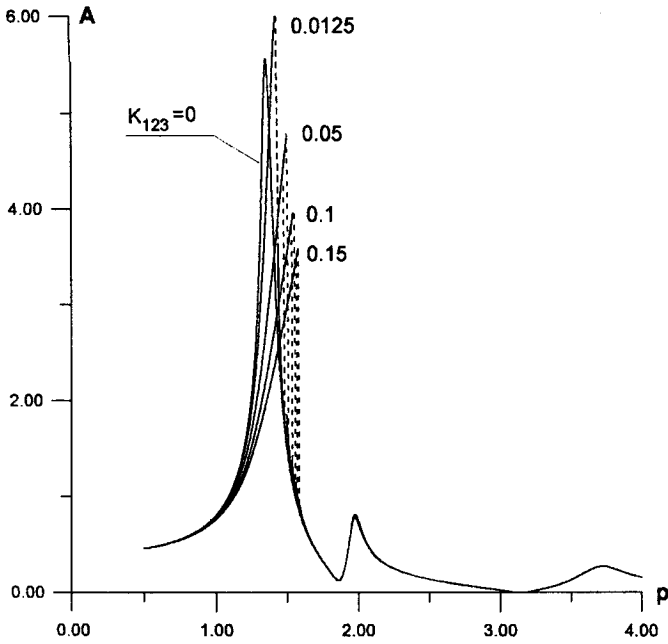


FIG. 8. Amplitude-frequency curves for displacements V_1 of the rigid body m_1 in the nonlinear Model II for $K_{123} = 0, 0.0125, 0.05, 0.1, 0.15$.

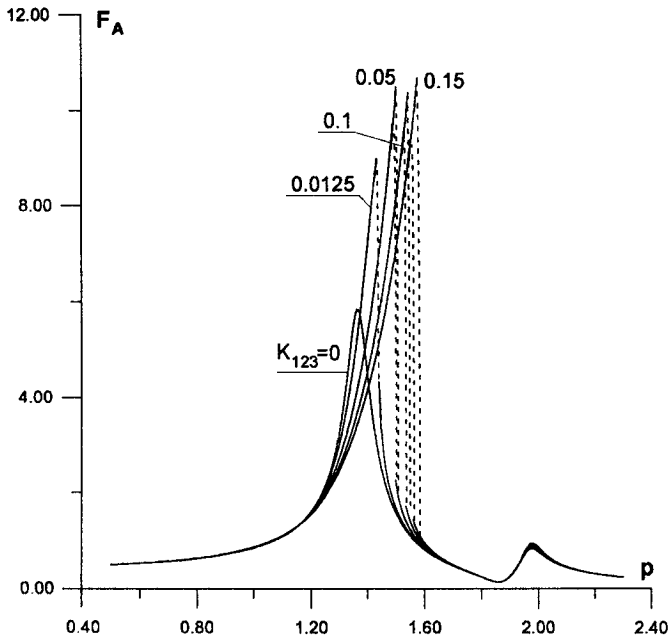


FIG. 9. Amplitude-frequency curves for dynamic force $F(V_1)$ in the nonlinear Model II for $K_{123} = 0, 0.0125, 0.05, 0.1, 0.15$.

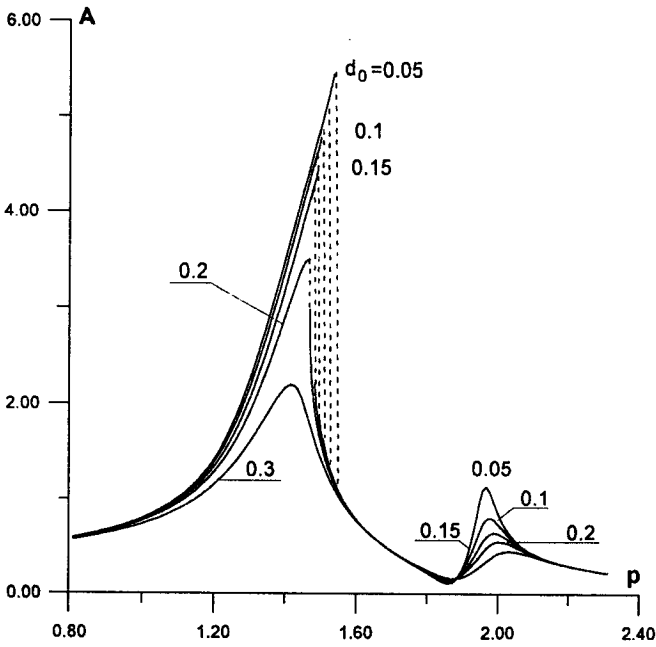


FIG. 10. Effect of damping on amplitudes of displacements V_1 in the nonlinear Model II for $d_0 = 0.05, 0.1, 0.15, 0.2, 0.3$ and $K_{123} = 0.05$.

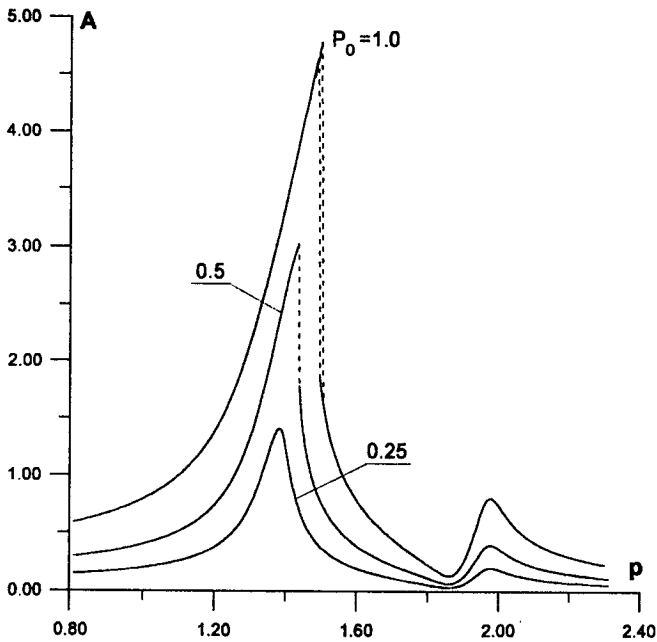


FIG. 11. Effect of amplitude P_0 of the external loading on amplitudes of displacements V_1 in the Model II with $P_0 = 0.25, 0.5, 1.0$ and $K_{123} = 0.05$.

in Figs. 10 and 11, respectively. From these figures it follows that the increase of damping leads to the decrease of the maximal amplitudes, and that with the decrease of P_0 the maximum amplitudes of V_1 also decrease. Linear cases are obtained for $d_0 = 0.3$, $P_0 = 1.0$ (Fig. 10) and for $P_0 = 0.25$, $d_0 = 0.1$ (Fig. 11). It should be pointed out that the linear model corresponding to the nonlinear Model II is discussed in [2] with $P_0 = 0.25$. The jump phenomena may be observed in the first resonant region. From all diagrams presented in Figs. 8–11 it follows that if $V_1 < 1.0$, the results for nonlinear models coincide with the results for the linear model.

6. FINAL REMARKS

The method utilizing the wave solution of the equations of motion can be an efficient tool in dynamic investigations of plane trusses with members subject to longitudinal deformations and loaded by long-lasting external forces. This concerns linear as well as nonlinear models.

Applications of this method in the linear cases is demonstrated in [2] on the example of two linear discrete-continuous models of portions of the plane truss consisting of members with continuously distributed mass and of rigid bodies located in the joints. In the present paper it is shown that the approach used in the paper [2] can be adopted for dynamic investigations of the nonlinear discrete-continuous models of the plane truss.

For both the nonlinear models discussed, the effect of local nonlinearity is observed in the first resonant region as the jump phenomenon typical for nonlinear discrete systems. The presented amplitude-frequency curves show not only the effect of the parameters representing the local nonlinearity, but they also allow to estimate the displacements at which the local nonlinearities can be neglected in the considered discrete-continuous models of the truss.

From the comparison of the appropriate amplitude-frequency diagrams for nonlinear Models I and II it follows that the change of the boundary conditions in the considered models does not have any significant effect on the amplitudes of the displacements, except the increase of the number of resonant regions. However, as it is shown in the paper [2], in numerous cross-sections of the truss members this effect is significant.

In the paper two simple models of the portions of plane trusses are discussed. The method used in the considerations can be easily applied to the study of more complex nonlinear models of plane trusses with longitudinally deformed members.

REFERENCES

1. J.M. GERE and W. WEAVER, *Analysis of framed structures*, D.Van Nostrand Company, Inc., New York 1965.
2. W. NADOLSKI and A. PIELORZ, *The use of elastic waves in dynamic investigations of plane truss members*, The Arch. of Mech. Engng., **43**, 105–123, 1996.
3. A. NIEMIERKO, *On the trusses* [in Polish], WKiŁ, Warsaw 1987.
4. W. GUTKOWSKI, J. BAUER and Z. IWANOW, *Explicit formulation of Kuhn-Tucker necessary conditions in structural optimization*, Computers and Structures, **37**, 753–758, 1990.
5. U. BERNHARD and W. HAUGER, *The propagation of waves in impact-loaded spatial trusses*, Arch. Appl. Mech., **63**, 556–566, 1993.
6. T.P. DESMOND, *Theoretical and experimental investigation of stress waves in junction of three bars*, J. Appl. Mech., **48**, 148–154, 1981.
7. J.P. LEE, *Elastic waves produced by longitudinal impact on system with symmetrically branched rods*, Int. J. Solids Structures, **8**, 699–707, 1972.
8. P. HAGEDORN, *Non-linear oscillations*, Clarendon Press, Oxford 1981.
9. A. PIELORZ, *Dynamic analysis of a nonlinear discrete-continuous torsional system by means of wave method*, ZAMM, **75**, 691–698, 1995.

POLISH ACADEMY OF SCIENCES

INSTITUTE OF FUNDAMENTAL TECHNOLOGICAL RESEARCH.

e-mail: apielorz@ippt.gov.pl

Received October 21, 1996.
